Journal of Power Sources 184 (2008) 691–694

Contents lists available at ScienceDirect

Journal of Power Sources

journal homepage: www.elsevier.com/locate/jpowsour

Short communication

Supercapacitive studies on amorphous MnO_2 in mild solutions

Chengjun Xu[a,b], Baohua Li[a], Hongda Du[a], Feiyu Kang[b,*], Yuqun Zeng[c]

[a] Advanced Materials Institute, Graduate School at Shenzhen, Tsinghua University, Shenzhen, Guangdong Province 518055, China
[b] Laboratory of Advanced Materials, Department of Materials Science and Engineering, Tsinghua University, Beijing 100084, China
[c] Amperex Technology Limited, Dongguan City, Guangdong Province 523080, China

ARTICLE INFO

Article history:
Received 21 January 2008
Received in revised form 25 March 2008
Accepted 1 April 2008
Available online 8 April 2008

Keywords:
MnO_2
Salt concentration
Cation activity
Supercapacitor
Aqueous electrolyte

ABSTRACT

Manganese dioxide has been synthesized by a self-reacting microemulsion method. The result of X-ray diffraction shows that lack of clear peaks and broadening of peaks indicate its amorphous nature. Typical cyclic voltammograms were measured in 0.5 mol L^{-1} Na_2SO_4 aqueous solution and the potential ranges were controlled from −0.5 to 0.5, from −0.65 to 0.65, and from −0.75 to 0.75 V versus Hg/Hg_2SO_4 at a sweep rate of 2 mV s^{-1}. Rectangular and symmetric image was observed between −0.5 and 0.5 V indicating high electrochemical reversibility in this potential and sweep rate.

The influence of cation species and concentration (activity) on electrochemical performances of MnO_2 is also discussed in this work. Cyclic voltammetric experiments have been performed between −0.5 and 0.5 V versus Hg/Hg_2SO_4 in Li_2SO_4, Na_2SO_4 and K_2SO_4 aqueous solutions with different salt concentrations ranging from 0.05 to 1 mol L^{-1}. The specific capacitance of MnO_2 was found to depend strongly on the cation concentration and species, and specific capacitance value will increase with the increase of cation concentration for all electrolytes. The logarithmic dependence of capacitance of MnO_2 on cation activity indicates that the charge storage for MnO_2 is involved in a fast redox reaction through cation insertion.

1. Introduction

Several metal oxides and hydroxides for example, those of Ni, Co, V, and Mn, have been studied extensively for high power redox supercapacitors applications [1–3]. Among these metal oxides, manganese dioxide (MnO_2) is one of the promising materials due to its availability, cost-effectiveness and non-toxicity. MnO_2 can show excellent pseudo-capacitive behavior in mild aqueous solutions and conduct a specific capacitance of 160 F g^{-1} [4–7]. However, this value is competitive with carbon supercapacitors, but falls far short of the 760 F g^{-1} obtained with hydrous RuO_2 [8].

The nanoscale design and synthesis of manganese dioxides is a key field for improving upon its electrochemical properties. Nanosized particles of manganese dioxide possess properties favorable for high power supercapacitor applications because those large ratio of surface to volume results in an increase in chemical and electrochemical activity. Electrodes made of nanosized manganese dioxides are expected to offer high levels of material utilization for supercapacitor application. Microemulsion is a route for synthesis of nanoparticles of several metals and metal oxides. The reactants are confined in a micro-nanodroplets of water dispersed in an organic medium, and emulsion is stabilized by a surface active agent. Reactions carried out in emulsion media produce nanoparticles [9]. However, it was a complicated, time-consuming and raw materials-wasting method because the emulsion of each reactant must be prepared before synthesis and the surfactants aren't involved in reaction.

In this study, the one step emulsion method was employed to prepare nanosized hydrous manganese dioxide. The advantages of manganese dioxide as pseudo-capacitor material are combined with the supremacy of the preparation technique to make a specific nanostructure of manganese dioxide so as to get the best electrochemical properties in neutral electrolyte systems.

In addition, the cation species and concentration of the electrolytes have a direct impact on the pseudo-capacitance of MnO_2. Alkaline cations (Li^+, Na^+ and K^+) are always used in the electrolytes for MnO_2 electrode. The detail information of alkaline cations is listed in Table 1 [10]. However, the role of cation species and concentration of the electrolytes for pseudo-capacitive behavior of MnO_2 electrode is necessary to be revealed. In this work, a tentative attempt has been made to concern the supercapacitive behavior of

---

* Corresponding author. Tel.: +86 10 6277 3752; fax: +86 10 6277 1160.
E-mail address: fykang@tsinghua.edu.cn (F. Kang).

0378-7753/$ – see front matter © 2008 Elsevier B.V. All rights reserved.
doi:10.1016/j.jpowsour.2008.04.005

Table 1
Ionic radii, ionic conductivity, and mobility at infinite diluted aqueous solution

	Li^+	Na^+	K^+
Size (Å)			
In crystals	0.69	1.02	1.38
In aqueous solution	6	4	3
Conductivity (10^{-4} m^2 S mol^{-1})	38.7	50.1	73.5
Mobility (10^{-8} m^2 s^{-1} V)	4.0	5.2	7.6

MnO_2 electrodes with the cation species and concentration (activity) of the electrolytes.

2. Experimental

The MnO_2 powder was synthesized by a simple one step microemulsion. A 0.1 mol L^{-1} (M) $KMnO_4$ aqueous solution was prepared by dissolving potassium permanganate (AR, 99%) in deionized water. Meanwhile 13.32 g surfactant of high purity sodium bis(2-ethylhexyl) sulfosuccinate (Aerosol-OT, AOT) was added in 300 mL *iso*-octane and stirred well to get an optically transparent AOT/*iso*-octane solution. Then 32.4 mL of 0.1 M $KMnO_4$ solution was added in AOT/*iso*-octane solution, and this solution was dispersed by ultrasound for 30 min to prepare a dark brown precipitate. The product was separated, washed copiously several times with double distilled water and ethanol, and dried at 80 °C for 12 h [11]. Powder X-ray diffraction (XRD) pattern of MnO_2 sample was obtained by using TW3040/60 diffractometer (Tanalygical Company, Holland), in which Cu Kα was used as the source. N_2 adsorption and desorption studies were carried out using ASA P2010 (Micromeritics Company) surface area analyzer.

Electrodes were prepared by mixing 70 wt% of MnO_2 powder as an active material with 20 wt% acetylene black and 10 wt% polytetrafluoroethylene (PTFE). 70 mg of MnO_2 powder and 20 mg of acetylene black were first mixed and dispersed in ethanol by ultrasound for 30 min. Then the ink was dried at 80 °C for 4 h to get dark mixed powder and 200 mg of PTFE aqueous solution (5 wt%) was added to get a paste. Then the paste was dried at 80 °C and a little of 1-methyl-2-pyrrolidinone (NMP) was added to get a rubber-like paste, which was cold rolled into thick films. Pieces of film with 5 mg weight, typically 1 cm^2 in size, were then hot-pressed at 80 °C under 100 MPa on a stainless steel mesh connected to a nickel wire.

Electrochemical tests were performed with an Im6e (Zahner) electrochemical station. A piece of platinum gauze and Hg/Hg_2SO_4 (in saturated K_2SO_4) were assemblied as counter and reference electrode. A cyclic voltammetric experiment was performed on an acetylene black electrode without MnO_2 and the charge capacitance of this electrode was found to be negligible (≈10 F g^{-1}). All the electrochemical measurements of MnO_2 electrodes were performed at 25 ± 1 °C.

3. Results and discussion

Fig. 1 shows the XRD pattern of as-prepared MnO_2 sample. It can be seen that the peak profile is broaden indicating its amorphous nature. Broad peaks at $2\theta = 37.0$ and 65.8 are clearly present and are indexable to α-MnO_2 (JCPDS No. 44-0141). The S_{BET} value of as-prepared MnO_2 determined from N_2 adsorption and desorption measurement, is 145.7 m^2 g^{-1} [11].

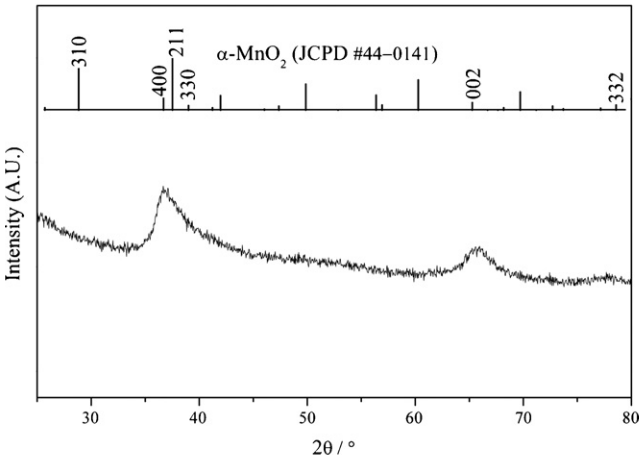

Fig. 1. X-ray diffraction pattern of MnO_2 sample.

Typical cyclic voltammograms (CVs) shown in Fig. 2, were measured in 0.5 M Na_2SO_4 aqueous solution and the potential ranges were from −0.5 to 0.5, from −0.65 to 0.65, and from −0.75 to 0.75 V versus $Hg/HgSO_4$ at a sweep rate of 2 mV s^{-1}. Rectangular and symmetric image was observed between −0.5 and 0.5 V indicating high electrochemical reversibility at the potential and sweep rate. As the potential range in which the CV test was conducted, was increased from ± 0.5 V to ± 0.75 V, at potentials above 0.5 V or below −0.5 V two pairs of relatively asymmetric peaks are clearly found. Similar results were reported for amorphous manganese oxides in the electrolytes using sodium sulfate as salt [7,12–14]. The maximum and minimum values of polarization potential of MnO_2 electrode are controlled by the reactions Mn(IV) to Mn(II) and Mn(IV) to Mn(VII), respectively, which are irreversible because of the solubility of both Mn(II) and Mn(IV) in water [11,13]. Therefore the potential must be controlled in the region, in which the reversible pseudo-capacitive behavior occurs.

The use of manganese dioxide, MnO_2, as an electrode material for electrochemical supercapacitors in mild solutions, is known to be based on the concept of a redox process associated with the insertion–extraction of cations in the electrolyte, for example Li^+, Na^+, or K^+ (A) into MnO_2 matrix:

$$MnO_2 + A^+ + e^- \leftrightarrow MnOOA \qquad (1)$$

The cation diffusion occurs via hopping of alkaline cations between H_2O or OH^- sites in MnO_2 matrix and this insertion–extraction is limited in a very thin layer (subsurface) of MnO_2 electrode. Meanwhile, the manganese oxidation state varies from IV to III for oxidized and reduced states of MnO_2 electrodes

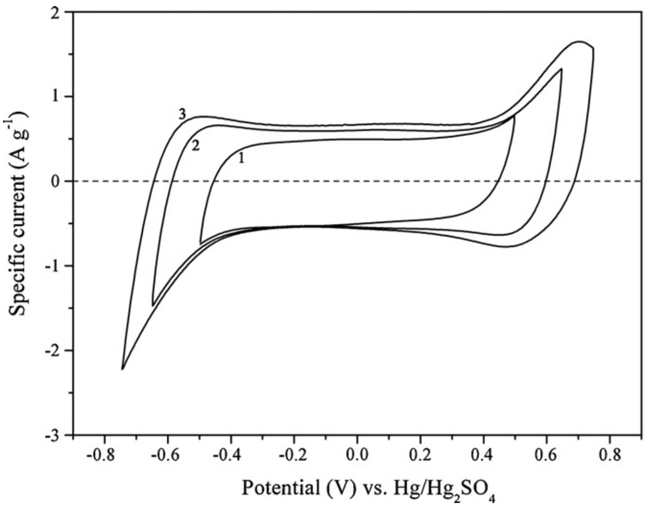

Fig. 2. Cyclic voltammograms of MnO_2 electrode with the upper and lower potential limits of CV equal to (1) (−0.5, 0.5); (2) (−0.65, 0.65); and (3) (−0.75, 0.75) V.

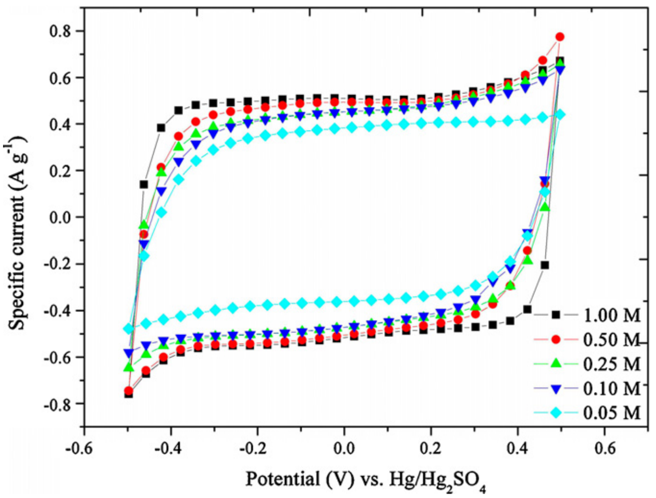

Fig. 3. The CVs of MnO_2 electrodes at 2 mV s^{-1} in Na_2SO_4 solutions with different salt concentrations.

during the insertion–extraction process to balance the charge, respectively [4,15–18]. Therefore, cation species and concentration will have a direct impact on the capacitance of MnO_2 electrode.

In order to monitor the effect of cation concentration and species on the pseudo-capacitance of MnO_2 electrodes, cyclic voltammetric experiments have performed between −0.5 and 0.5 V versus Hg/Hg_2SO_4 in Li_2SO_4, Na_2SO_4 and K_2SO_4 electrolytes with different salt concentrations ranging from 0.05 to 1 M. For the experiments of controlling cation concentration, the pH value of electrolyte was kept at ca. 6.0, and the proton concentration was far lower than the alkaline cation concentration in electrolytes. Fig. 3 shows the CVs of MnO_2 electrodes at 2 mV s^{-1} in Na_2SO_4 electrolytes with different salt concentrations. All images are rectangular, which shows MnO_2 possess good supercapacitive properties in Na_2SO_4 electrolytes with different salt concentrations.The specific capacitance (SC) of electroactive material can be estimated using half integrated area of the CV curve to obtain the charge (Q), and subsequently dividing the charge by the mass of the active material (m) and the width of the potential window (ΔV),

$$\mathrm{SC} = \frac{Q}{\Delta V m} \tag{2}$$

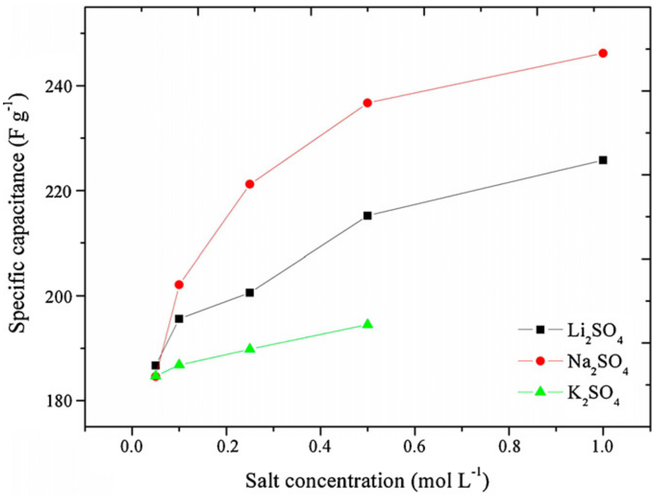

Fig. 4. Dependence of SC values on salt concentrations at sweep rate of 2 mV s^{-1}.

Fig. 4 shows the dependence of SC values of MnO_2 electrode and salt concentration in Li_2SO_4, Na_2SO_4 and K_2SO_4 electrolytes at a sweep rate of 2 mV s^{-1}. For all electrolytes, the specific capacitance increases as the cation concentration increased.

Considering the charging–discharging reaction of MnO_2 electrode in electrolytes (Eq. (1)), the rate law for charging–discharging step as an elementary reaction could be written as:

$$\text{Charging rate} = \frac{dq}{dt} = k_1[A^+] \tag{3}$$

where q is the charge, t is time, k_1 is the charging rate constant, A^+ is Li^+, Na^+ or K^+, and $[A^+]$ is cation concentration. The charging rate should be equal to the cation adsorption rate ($d[A^+]/dt$) for the charge neutrality of the charging reaction. Hence the charging–discharging rate can be written as:

$$\frac{dq}{dt} = \frac{d[A^+]}{dt} = k_1[A^+] \tag{4}$$

The differential equation $d[A^+]/dt = k_1[A^+]$, thus has the solution: $\ln[A^+] = k_1 t$. For the charging–discharging processes of an electrochemical capacitor, the rate of charging of q with an arbitrary sweep rate (v) is given by $dq/dt = v\,dC/dt$ [10]. Hence, the capacitance is expected to show the logarithmic dependence on the cation concentration, i.e. pA ($-\log[A^+]$). However, for a real solution with high concentration containing strong electrolyte such as Li_2SO_4, Na_2SO_4, or K_2SO_4, the cation activity must be introduced to replace cation concentration in order to represent the real cation concentration being involving in the electrochemical reaction: $a = f_i c$, where a is ion activity, f_i is activity coefficient, and c is ion concentration. Activity coefficient (f_i) can be calculated according to Debye–Hückel equation:

$$-\log f_i = \frac{A z_i^2 I^{1/2}}{(1 + B\mathring{a} I^{1/2})} \tag{5}$$

where f_i is activity coefficient, I is ionic strength, z_i is ion charge, A and B are coefficient, and $\mathring{a}$ is hydrated ion size of the cation (seen in Table 1.). At 25 °C in aqueous solutions, A and B are 0.5115 and 0.3291, respectively [19]. Ionic strength (I) of Li_2SO_4, Na_2SO_4 and K_2SO_4 electrolytes with different concentrations, shown in Table 2, can be calculated from equation:

$$I = 0.5(c_+ z_+ + c_- z_-) \tag{6}$$

where c_+ and c_- are the concentration of cation and anion, and z_+ and z_- are the charge of cation and anion, respectively. Therefore, based on above data, the activity coefficient can be calculated from Eq. (5), thus cation activity is also obtained. The calculated activity coefficient and cation activity are shown in Table 2.

The Eqs. (3) and (4) must be written by replacing cation concentration ($[A^+]$) by cation activity (a) as:

$$\text{Charging rate} = \frac{dq}{dt} = k_1 a \tag{7}$$

and

$$\frac{dq}{dt} = \frac{da}{dt} = k_1 a \tag{8}$$

Hence the capacitance is expected to show the logarithmic dependence on the cation activity, i.e. pA_a ($-\log a_A$),

$$C = k\,pA_a + b \tag{9}$$

The capacitances of MnO_2 electrodes depending on the cation activities are plotted as functions of pLi_a ($-\log a_{Li}$), pNa_a ($-\log a_{Na}$) and pK_a ($-\log a_K$) as shown in Fig. 5. The capacitances show the linear dependence on the pLi_a, pNa_a and pK_a. This linear dependence implies that the charging–discharging process is mainly controlled by cation insertion–extraction of cations and the charging process

Table 2
Activity coefficient of the cation, ionic strength and cation activity

Salt concentration (mol L^{-1})		1	0.5	0.25	0.1	0.05
Ionic strength (I)		3	1.5	0.75	0.3	0.15
Cation concentration (mol L^{-1})		2	1	0.5	0.2	0.1
f_i	Li^+	0.6303	0.6558	0.6862	0.7335	0.7722
	Na^+	0.5369	0.5757	0.6209	0.6874	0.7393
	K^+	–	0.5106	0.5770	0.6579	0.7189
a_i (mol L^{-1})	Li^+	1.2606	0.6558	0.3431	0.1467	0.0772
	Na^+	1.0738	0.5757	0.3104	0.1375	0.0739
	K^+	–	0.5106	0.2885	0.1316	0.0719

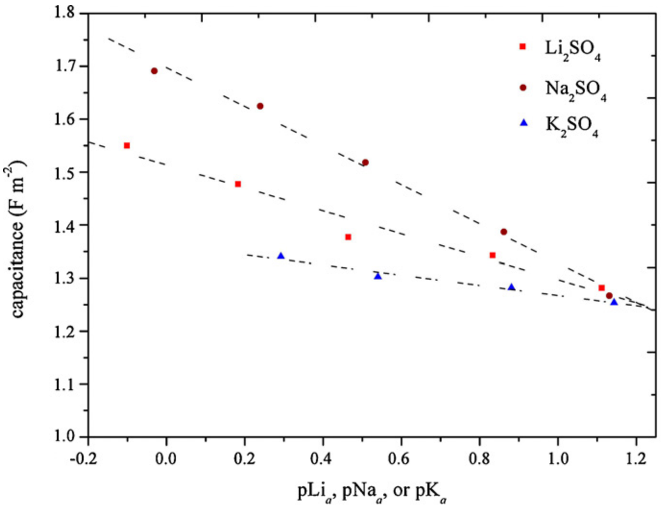

Fig. 5. Dependence of specific capacitance of MnO_2 on pLi_a ($-\log a_{Li}$), pNa_a ($-\log a_{Na}$) and pK_a ($-\log a_K$).

is the first-order reaction with respect to the cation activity of the electrolyte.

The slopes of the plot of capacitances versus the pLi_a, pNa_a and pK_a are −0.21, −0.34 and −0.10 in the linear range of pLi_a, pNa_a and pK_a, respectively. The largest value of the slope, which represents the fastest rate of charge and discharge, is observed in Na_2SO_4 electrolytes and the flattest slope is obtained in K_2SO_4 electrolyte.

The whole charging–discharging process of MnO_2 may mainly involve: (i) cation transport in the electrolyte; (ii) adsorption–desorption of cation at the surface sites of MnO_2 electrode, which may be dependent on the ion size and the dehydration–hydration rate; and (iii) cation extraction–insertion into solid MnO_2 matrix.

Therefore, the charging–discharging rate can be affected by the size of the cation, the size of the hydrated cation, the mobility of the cation, and the adsorption–desorption rate. However, it is known if the cation size is way too big such as K^+, it is difficult to squeeze and diffuse in the MnO_2 matrix. Since diffusion of cation in subsurface (a very thin layer) of solid MnO_2 electrode is more difficult than in an aqueous solution even its hydrated form need travel from far away in the solution to the surface of MnO_2 electrode, therefore, a flattest slope is expected for K^+ due to its very large ion size. On the other hand, if the size of the cation is very small such as Li^+, which means a large hydrated size, cation transport in the solution would meet more resistance and the dehydration–hydration rate would be slowed down dramatically. With a moderate bare ion size and hydrated size, Na^+ ion may possess a moderate diffusion rate in solid MnO_2 matrix, a moderate adsorption–desorption rate, and a moderate mobility in aqueous solutions, which seems to be the important factors to the large capacitance and fast charging/discharging rate. However, further experiment is necessary to determine diffusion properties of the cations.

4. Conclusion

Manganese dioxide was prepared by a new simple method. The result of XRD pattern shows its amorphous nature. The electrodes of MnO_2 show rectangular and symmetric CV curves between −0.5 and 0.5 V (vs. $Hg/HgSO_4$) in Na_2SO_4 electrolyte with salt concentration ranging from 0.05 to 1 mol L^{-1}. The capacitances of MnO_2 electrodes were monitored as a function of the concentration of cations. The logarithmic dependence of capacitance on the activity of cations in electrolytes indicates that the charging–discharging process is mainly controlled by the insertion–extraction of cations.

Acknowledgements

This work was supported by the Natural Science Foundation of China under Grant No. 50632040. The authors would like to appreciate SAE Magnetic Ltd. for their supports.

References

[1] T.-C. Liu, W.G. Pell, B.E. Conway, Electrochim. Acta 44 (1999) 2829.
[2] H.Y. Lee, J.B. Goodenough, J. Solid State Chem. 148 (1999) 81.
[3] V. Srinivasan, J.W. Weidner, J. Power Sources 108 (2002) 15.
[4] T. Brousse, M. Toupin, R. Dugas, L. Athouël, O. Crosnier, D. Bélanger, J. Electrochem. Soc. 153 (2006) A2171.
[5] R.N. Ready, R.G. Ready, J. Power Sources 132 (2004) 315.
[6] V. Subramanian, H.W. Zhu, B.Q. Wei, J. Power Sources 159 (2006) 361.
[7] A. Zolfaghari, F. Ataherian, M. Ghaemi, A. Gholami, Electrochim. Acta 52 (2007) 2806.
[8] J.P. Zheng, Electrochem. Solid State Lett. 2 (1999) 359.
[9] S. Devaraj, N. Munichandraiah, J. Electrochem. Soc. 154 (2007) A808.
[10] S. Wen, J.-W. Lee, I.-H. Yeo, J. Park, S.-I. Mho, Electrochim. Acta 50 (2004) 8495.
[11] C. Xu, B. Li, H. Du, F. Kang, Y. Zeng, J. Power Sources 108 (2008) 664–670.
[12] V. Khomenko, E. Raymudo-Piñero, F. Béguin, J. Power Sources 153 (2006) 183.
[13] M. Toupin, T. Brousse, D. Bélanger, Chem. Mater. 14 (2002) 3950.
[14] C.-C. Hu, T.-W. Tsou, Electrochem. Commun. 4 (2002) 107.
[15] S.C. Pang, M.A. Anderson, T.W. Chapman, J. Electrochem. Soc. 147 (2000) 44.
[16] M. Ghaemi, F. Ataherian, A. Zolfaghari, S.M. Jafari, Electrochim. Acta 53 (2008) 4607.
[17] J. Rishpon, S. Gottesfeld, J. Electrochem. Soc. 131 (1984) 1960.
[18] M. Toupin, Thierry, D. Bélanger, Chem. Mater. 16 (2004) 3184.
[19] J.A. Dean, Lange's Handbook of Chemistry, McGRAWHILL, 1992.